Survival probability of atmospheric new particles: closure between theory and measurements from 1.4 to 100 nm

Runlong Cai[1,*], Chenjuan Deng[2], Dominik Stolzenburg[1], Chenxi Li[3], Junchen Guo[2], Veli-Matti Kerminen[1], Jingkun Jiang[2], Markku Kulmala[1,4], Juha Kangasluoma[1,5]

[1]Institute for Atmospheric and Earth System Research / Physics, Faculty of Science, University of Helsinki, Helsinki, 00014, Finland
[2]State Key Joint Laboratory of Environment Simulation and Pollution Control, School of Environment, Tsinghua University, Beijing, 100084, China
[3]School of Environmental Science and Engineering, Shanghai Jiao Tong University, Shanghai, 200240, China
[4]Aerosol and Haze Laboratory, Beijing Advanced Innovation Center for Soft Matter Science and Engineering, Beijing University of Chemical Technology, Beijing, 100029, China
[5]Karsa Ltd., A. I. Virtasen aukio 1, Helsinki, 00560, Finland

Correspondence to: Runlong Cai (runlong.cai@helsinki.fi)

Abstract. The survival probability of freshly nucleated particles governs the influences of new particle formation (NPF) on atmospheric environments and the climate. It characterizes the probability of a particle to avoid being scavenged by the coagulation with pre-existing particles and other scavenging processes before the particle successfully grows up to a certain diameter. Despite its importance, measuring the survival probability has been challenging, which limits the knowledge of particle survival in the atmosphere and results in large uncertainties in predicting the influences of NPF. Here we report the proper methods to retrieve particle survival probability of the measured aerosol size distributions at different particle sizes. Using diverse aerosol size distributions from urban Beijing, the Finnish boreal forest, a chamber experiment, and aerosol kinetic simulations, we demonstrate that each method is valid for a different type of aerosol size distributions whereas misapplying the conventional methods to banana-type NPF events may underestimate the survival probability. Using these methods, we investigate the consistency between the measured survival probability of new particles and the theoretical survival probability against coagulation scavenging predicted using the measured growth rate and coagulation sink. With case-by-case and time- and size-resolved analysis of long-term measurement data from urban Beijing, we find that although both the measured and theoretical survival probabilities are sensitive to uncertainties and variations, they are, on average, consistent with each other for new particles growing from 1.4 nm (the cluster size) to 100 nm.

1 Introduction

30 As one of the largest sources of uncertainties in the climate prediction, atmospheric aerosol plays a key role in diverse environments. New particle formation (NPF) via vapor nucleation and subsequent growth (Kulmala et al., 2004; Zhang et al., 2012; Kulmala et al., 2013) is a key phenomenon associated with the atmospheric aerosol system, contributing majorly to the number concentrations of aerosols and cloud condensation nuclei (Kuang et al., 2009; Gordon et al., 2017). To reach a relatively long atmospheric residence time and exert significant influences on atmospheric environments, freshly nucleated

35 particles need to grow fast beyond the smallest size range (e.g., sub-10 nm), in which they are most likely to be scavenged by pre-existing aerosols (McMurry, 1983; Kulmala et al., 2001). Hence, the fraction of freshly nucleated particles that survive the scavenging after a certain growth process, characterized by the survival probability, is a decisive factor for the atmospheric influences of NPF.

Although the formation rate (J) and growth rate (GR) of new particles have been often used to characterize NPF events

40 (Kulmala et al., 2012; Kerminen et al., 2018), the survival probability is an irreplaceable important parameter in NPF studies. J and GR can connect the gaseous precursors and new particles, providing information on the formation and growth mechanisms. In terms of atmospheric influences, however, it is the total number of new particles formed during NPF and their survival probabilities that determine the contribution of NPF to the number of large particles. While the total number of new particles can be readily obtained by integrating J over time, predicting the survival probability requires the information on the

45 sink of particles in addition to GR. Although several studies computed the survival probability using the ratio of J at different particle sizes, we will show below that this method is only valid for a certain type of NPF events.

The knowledge of particle survival probability in the real atmosphere is rather limited despite its importance. On one hand, theoretical survival probabilities predicted using GR and the coagulation sink (CoagS) of new particles have been widely used in regional and global models, bridging the gap between the size of freshly nucleated particles and the smallest size bin/mode

50 in the model (Kerminen and Kulmala, 2002; Lehtinen et al., 2007). On the other hand, however, there have been only a limited number of studies reporting the measured survival probabilities retrieved from aerosol size distributions (e.g., Weber et al., 1997; Kuang et al., 2009; Kulmala et al., 2017). The limited information from measurements is the main obstacle for validating the modelling results and understanding particle survival. For instance, Kulmala et al. (2017) reported that for sub-3 nm particles in polluted megacities, the theoretically predicted survival probability could not explain the measured value with a

55 deviation of several orders of magnitude, urging further investigations of the survival of freshly nucleated particles.

Retrieving the size-resolved survival probability from measured aerosol size distributions is the first step to address the consistency problem between measurements and theory, yet it has been challenging. The challenge mainly comes from the difficulty to track the growth and survival of individual particles or an aerosol population, as the measured particles are a sum of the survived particles and other newly formed particles. Therefore, one has to retrieve survival probability from

60 measurements based other parameters instead of the number of the growing particles. Weber et al. (1997) used the

concentration of gaseous sulfuric acid and the theoretical survival probability to estimate the total concentration (N) of particles larger than 3 nm, which essentially approximated the measured survival probability with the ratio of N at different time. Kerminen and Kulmala (2002) derived the theoretical survival probability of a strictly monodisperse aerosol population and concluded that the survival probability should be equal the ratio of J at different sizes. Kuang et al. (2009) derived a semi-analytical formula for $n = \mathrm{d}N/\mathrm{d}d_\mathrm{p}$ of an aerosol population with the influence of time-dependent source and sink terms, where n is the aerosol size distribution in the linear scale of particle size. The ratio of n at different sizes was taken as the survival probability. However, the derivations and validations of these formulae using N, J, and n may need further discussion. Here we demonstrate, that each formula is valid for only a certain type of NPF events and it may report substantially biased survival probabilities for other events. These potential biases demand for advances in the methods to retrieve the measured survival probability.

In this study, we report the proper formulae to retrieve the measured survival probability of atmospheric new particles. In addition to conventional formulae based on J and n, we propose a new formula based on $n_\mathrm{log} = \mathrm{d}N/\mathrm{dlog}d_\mathrm{p}$ to retrieve the measured survival probability from a growing aerosol population (e.g., in a banana-type NPF event). The performance of these formulae with different types of size distributions are tested using benchmark simulations based on aerosol kinetics and measurements from the real atmosphere, showing that these formulae are valid for their corresponding types of aerosol size distributions.

We then use the proper formulae to investigate the consistency between the measured and theoretical survival probabilities. Using data from long-term measurements in urban Beijing, a case study measured from a Finnish boreal forest site, and a chamber experiment, we performed case-by-case and time- and size-resolved analysis of particle survival probabilities. The results show that despite the large variations and high sensitivity in the survival probability, especially for sub-5 nm particles, the measured survival probability of new particles growing from 1.4 nm (electrical mobility diameter) to 100 nm can on average be explained by theory.

2 Theory

2.1 Definition of survival probability

The survival probability of a growing new particle is the probability that the particle at an initial diameter (d_p1, nm) will grow to a specified diameter (d_p2) before it is scavenged (Weber et al., 1997; Pierce and Adams, 2007). For a growing monodisperse aerosol population containing a large number of particles in a steady environment, the survival probability is equal to the fraction of particles successfully growing from d_p1 to d_p2 against the scavenging, i.e.,

$$P\left(d_\mathrm{p1} \rightarrow d_\mathrm{p2}\right) \equiv \frac{N_2\left[d_\mathrm{p2}(t_2)\right]}{N_1\left[d_\mathrm{p1}(t_1)\right]} \tag{1}$$

where P (-) is the survival probability, N (cm^{-3}) is the particle number concentration, t (s) is time, and the subscript indicates the particle size and number concentration of the aerosol population corresponding to a certain time. Equation 1 emphasizes that the survival probability is defined for the same aerosol population and that the aerosol concentration is not affected by atmospheric processes of transport, mixing, dilution, etc.

2.2 Theoretical survival probability

The theoretical survival probability, referred to as P_{theo} below, can be predicted using time-and-size-dependent scavenging losses. For freshly nucleated atmospheric new particles, scavenging losses are usually governed by Brownian coagulation (Kulmala et al., 2001). With a reasonable approximation that particles in the growing population share the same time-and-size-dependent coagulation sink, the theoretical probability against coagulation scavenging can be computed by integrating CoagS as a function of particle size and time, i.e.,

$$P_{\text{theo}}\left(d_{\text{p1}} \to d_{\text{p2}}\right) = 1 - \frac{\int_{t_1}^{t_2} \text{CoagS}[d_{\text{p}}(t)] \cdot N[d_{\text{p}}(t)] \cdot \mathrm{d}t}{N_1} \tag{2}$$

Further assuming that particles share the same time-and-size-dependent GR (nm s^{-1}) and substituting $\mathrm{d}t = \mathrm{d}d_p/\text{GR}$ and $N = N_1 \cdot P_{\text{theo}}$ into the derivate of Eq. 2, one can obtain $\mathrm{d}P_{\text{theo}}/P_{\text{theo}} = -\mathrm{d}t \cdot \text{CoagS}/\text{GR}$. Integrating this differential formula yields Eq. 3 in which P is expressed as a function of d_{p},

$$P_{\text{theo}}\left(d_{\text{p1}} \to d_{\text{p2}}\right) = \exp\left[\int_{d_{\text{p1}}}^{d_{\text{p2}}} -\frac{\text{CoagS}(d_{\text{p}})}{\text{GR}(d_{\text{p}})} \cdot \mathrm{d}d_{\text{p}}\right] \tag{3}$$

Equation 3 can be further simplified with predetermined size dependencies of CoagS (s^{-1}) and GR, as have been given in previous studies (Weber et al., 1997; Kerminen and Kulmala, 2002; Lehtinen et al., 2007; Korhonen et al., 2014). These simplified formulae can be readily applied to compute P_{theo} without CoagS and GR for each d_{p}, yet in this study we use Eqs. 2 and 3 for better accuracy.

2.3 Measured survival probability

Different from the theoretical survival probability predicted using CoagS and GR (Eqs. 2 and 3), the measured survival probability is retrieved from the size distribution of growing new particles. Because of the challenges in tracking the same growing aerosol population against other freshly nucleated or pre-existing particles, it is practically difficult to use the definition of the survival probability in Eq. 1 for atmospheric measurements. As aforementioned, particle formation rate J (cm^{-3} s^{-1}) (Kerminen and Kulmala, 2002) and linear size-scale distribution $n = \mathrm{d}N/\mathrm{d}d_{\text{p}}$ (cm^{-3} nm^{-1}) (Kuang et al., 2009) have been used as the parameters to retrieve particle survival probability from a growing aerosol population. In this study, however, we find that J and n are valid for steady-state and quasi-steady-state size distributions but may not for a growing aerosol population,

whereas the logarithmic size-scale $n_{\log} = dN/d\log_{10}d_p$ is a promising parameter for a growing aerosol population. The
corresponding formulae for retrieving the measured survival probability are given in Eqs. 4-6:

$$P(d_{p1} \rightarrow d_{p2}) = \frac{J_2(t_2)}{J_1(t_1)} \tag{4}$$

$$P(d_{p1} \rightarrow d_{p2}) = \frac{n_2(t_2)}{n_1(t_1)} \tag{5}$$

$$P(d_{p1} \rightarrow d_{p2}) = \frac{n_{\log,2}(t_2)}{n_{\log,1}(t_1)} \tag{6}$$

where the subscripts 1 and 2 indicate the diameters d_{p1} and d_{p2}, respectively, at which J, n, and $n_{\log}$ are evaluated. For the
convenience of illustration, we refer the survival probabilities retrieved using J, n, and $n_{\log}$ as P_J, P_n, and $P_{n\log}$, respectively.

2.4 Theoretical analysis of the measured survival probability

Here we present theoretical analysis on the validity of Eqs. 4-6 using two ideal types of aerosol size distributions. First, for a
growing aerosol population, which is assumed to follow a lognormal distribution, the survival probability can be expressed as
Eq. 7 according to the definition in Eq. 1.

$$P(d_{p1} \rightarrow d_{p2}) \equiv \frac{N_2[d_{p2}(t_2)]}{N_1[d_{p1}(t_1)]} = \frac{n_{\log,2}(t_2)}{n_{\log,1}(t_1)} \cdot \frac{\ln(\sigma_{g,2})}{\ln(\sigma_{g,1})} \tag{7}$$

where $n_{\log}$ is the value at the distribution peak and σ_g is geometric standard deviation of aerosol size distribution.

For a growing aerosol population in the atmosphere, it is an empirical fact that the geometric standard deviation usually
maintains at relatively constant level. Figure 1 shows an example of banana-type NPF events with a clear growth pattern of
new particles from 5 nm to 60 nm. Although there was minor variations in the geometric standard deviation, the maximum $n_{\log}$
was relatively constant after normalizing the change in N. This indicates that neglecting the $\ln(\sigma_{g,2})/\ln(\sigma_{g,1})$ term in Eq. 7 would
introduce only a minor uncertainty and hence $P_{n\log}$ in Eq. 6 could provide a good estimate of the survival probability of particles
in this growing population. In contrast, n was significantly broadened as d_p increases and the maximum n decreased due to this
broadening. This indicates that P_n in Eq. 5 would underestimate survival probability of the growing aerosol population. Since
$J = n \cdot GR$, P_J in Eq. 4 would also underestimate the survival probability.

=====================
Figure 1
=====================

We then consider another type of ideal aerosol size distribution, for which the n of freshly nucleated particles are at a steady-
state. The steady-state refers to a condition at which the time derivative of n is negligible, i.e.,

$$\frac{\partial n(d_{\mathrm{p}})}{\partial t} = -\frac{\partial J(d_{\mathrm{p}})}{\partial d_p} - \mathrm{CoagS}(d_{\mathrm{p}}) \cdot n(d_{\mathrm{p}}) \approx 0 \tag{8}$$

where the $\partial J(d_{\mathrm{p}})/\partial d_p$ term characterizes the flux of growing particles through d_{p}.

The formulae for the measured survival probability of particles with this steady-state distribution can be theoretically derived. Substituting $n = J/\mathrm{GR}$ into Eq. 8 and integrating from d_{p1} to d_{p2} yields the relationship between J and CoagS/GR,

$$\frac{J_2(t)}{J_1(t)} = \exp\left[\int_{d_{\mathrm{p1}}}^{d_{\mathrm{p2}}} -\frac{\mathrm{CoagS}(d_{\mathrm{p}})}{\mathrm{GR}(d_{\mathrm{p}})} \cdot \mathrm{d}d_{\mathrm{p}}\right] \tag{9}$$

Comparing Eqs. 3 and 9, one can readily conclude that J_2/J_1 is equal to the survival probability of particles with a steady-state

140   size distribution. With a size-independent GR, n_2/n_1 is also equal to the survival probability, i.e.,

$$P(d_{\mathrm{p1}} \to d_{\mathrm{p2}}) = \frac{J_2(t)}{J_1(t)} \tag{10}$$

$$P(d_{\mathrm{p1}} \to d_{\mathrm{p2}}) = \frac{n_2(t)}{n_1(t)} \cdot \frac{\mathrm{GR}_2(t)}{\mathrm{GR}_1(t)} \approx \frac{n_2(t)}{n_1(t)} \tag{11}$$

It worth emphasizing that although Eqs. 10-11 look very similar to Eqs. 4-5, there is a conceptual difference between them. This difference lies in the view of the two ideal aerosol size distributions. For the growing aerosol population, we track the time evolution of the aerosol size distribution from a Lagrangian point of view in the particle size space (Eqs. 4-6). For the steady-state aerosol size distribution, the measured size distribution is the sum of particles formed at different time. Instead of

145   tracking the time evolution, we focus on the particle growth fluxes through certain size bins at the same moment and then derive the relationship between the measured size distribution and the survival probability (Eqs. 10-11).

Summarizing the analysis above, $P_{n\log}$ is expected to be valid for a growing aerosol population, whereas P_J and P_n are expected to be valid for a steady-state distribution.

3 Methods

150   ### 3.1 Simulation

A sectional model based on aerosol kinetics was used as a benchmark to generate aerosol size distributions and test the formulae for survival probability computation. The evolving aerosol size distribution was simulated by numerically solving aerosol population balance equations, which accounts for new particle formation, particle condensational growth, the coagulation sink of particles, and self-coagulation of new particles. Detailed information on this model have been described

155   previously (Li and Cai, 2020). We validated the accuracy of the sectional model using a discrete model, ensuring that the bias caused by numerical diffusion was negligible under the simulation conditions. For the convenience of discussion, we used

time-independent external coagulation sinks for particles in these simulations. A growth enhancement factor for particle growth (Kuang et al., 2010) was used as an input parameter to generate size-dependent grow rates. The simulation conditions are summarized in Table 1.

160

===================
Table 1
===================

3.2 Measurements

We investigated the survival probability of new particles and the validity of different methods for survival probability

165 computation using data measured from urban Beijing and a Finnish boreal forest site. The long-term NPF data for urban Beijing was measured at the BUCT site (Liu et al., 2020), which was located on the west campus of Beijing University of Chemical Technology and close to the west 3rd Rind Road of Beijing. Despite the high coagulation sink of new particles in urban Beijing (Cai et al., 2017b), intensive NPF events have been frequently observed. We used the data measured from Jan 16th to Dec 26th, 2018 in Beijing to represent NPF events in polluted megacities and analyzed a total of 65 NPF event days with clear patterns

170 of new particle formation and growth. The NPF event measured on Apr. 11th, 2020 from a relatively clean environment at the SMEAR II station at Hyytiälä, Finland (Hari and Kulmala, 2005) was analyzed as a case study. We also analysed an NPF experiment measured in the Cosmics Leaving Outdoor Droplets (CLOUD) chamber at the European Center for Nuclear Research (CERN) (Kirkby et al., 2011; Duplissy et al., 2016). In that experiment, gaseous precursor (α-pinene, isoprene, and ozone) concentrations were kept constant and NPF was initiated by a sudden increase in ion concentrations in the chamber

175 (Heinritzi et al., 2020), yielding a steady-state aerosol size distribution during NPF.

The aerosol size distributions in the Beijing atmosphere were measured using a diethylene glycol scanning mobility particle spectrometer (DEG-SMPS) (Jiang et al., 2011) and a particle size distribution system (PSD) (Liu et al., 2016). The DEG-SMPS covered the size range of 1-6.5 nm (electrical mobility diameter, same below), and it was deployed with a core sampling device (Fu et al., 2019) and a miniature cylindrical differential mobility analyzer (Cai et al., 2017a) to improve the sampling

180 and classification of particles in this size range. The PSD was used to measure particles ranging from 3 nm to 10 µm. The aerosol size distributions at Hyytiälä were measured using a DMA-train (Stolzenburg et al., 2017) and a twin differential mobility particle spectrometer (Aalto et al., 2001), covering the diameter ranges of 1.8-8 nm and 3-1000 nm, respectively. At CLOUD, the aerosol size distributions were measured by the DMA-train (1.8-8 nm) and a TSI nano-SMPS (Model 3982, 2-64 nm). All these instruments obtained the size information of aerosols based on the electrical mobility classification, which

185 could provide a relatively good sizing accuracy especially for freshly nucleated particles.

3.3 Data analysis

The formation rate J, CoagS, and GR along the growth trajectories of new particles were determined to compute the survival probability of atmospheric new particles. J was retrieved using a population balance method with improved accuracy for NPF in polluted environments (Cai et al., 2017a). Time-and-size dependent CoagS was computed using the measured particle size distribution (Kulmala et al., 2001).

We tested the performance of different methods in different environments in order to minimize the uncertainties in the retrieved GR. For urban Beijing, we found a systematic difference between the GR estimated using appearance time method (Lehtipalo et al., 2014; Cai et al., 2021) and the mode-fitting method (Kulmala et al., 2012; Deng et al., 2020) for sub-5 nm particles, which has been reported previously (Qiao et al., 2021; Deng et al., 2021). Such a difference is likely due to the influences of the continuous formation of freshly nucleated particles and primary emissions of particles. The mode fitting method tracks the growth of peak diameter of a new particle mode. However, the fitted mode is a sum of the growing particles and freshly nucleated particles and hence the apparent growth of the fitted mode is slower than the growing mode. Consequently, the mode-fitting method tends to underestimate the GR for sub-5 nm particles (Cai et al., 2022). Hence, we used the 50 % appearance time method to calculate the GR for sub-5 nm particles and applied a GR-based correction when computing P_{theo}. For Hyytiälä, the GR retrieved using the maximum concentration method (Kulmala et al., 2012) that finds the time corresponding to the maximum particle concentration in each size bin. The GR retrieved using the maximum concentration method was consistent with that retrieved using the 50 % appearance time method. We did not use the appearance method directly because it does not track the growth trajectory of new particles.

The measured survival probabilities of atmospheric new particles were computed using Eqs. 4-6. According to our simulation results, we determined n and n_{log} for each particle size in Eqs. 5-6 along smoothed growth trajectories and J in Eq. 4 as the daily maximum J for each size bin.

The P_{theo} for atmospheric new particles was computed using Eq. 2, with the CoagS determined along the growth trajectory and the concentration of new particles numerically solved by iteration. This approach is equivalent to using Eq. 3 with time-and-size dependent CoagS and GR.

To compare the theoretical and measured survival probabilities from long-term measurements in urban Beijing, we first computed their values for each NPF event. Considering the fact that the validity of the formulae to retrieve the measured survival probability in Eqs. 4-6 is based on the homogeneity of the system, we compared the medians of the theoretical and measured values. The medians were first computed for each size bin, and the overall median survival probabilities were then reconstructed by integrating the size-resolved values from 1.4 nm to 100 nm. In this way, we minimized the influences of atmospheric variations and preserved the non-linearity of the survival probability as a function of GR and CoagS.

4 Results and discussion

4.1 Validity of P_J, P_n, and $P_{n\log}$ for different types of NPF events

We first test the methods to retrieve the survival probability of particles in a growing aerosol population against coagulation scavenging. For a simulated system without particle sources from nucleation, primary emissions, etc., (Fig. 2a), the "true" survival probability can be retrieved with N using the definition in Eq. 1 since all the particles are from the same population. P_{theo} can be predicted using Eqs. 2-3 with an approximation that the particles in this growing population share the same size-dependent CoagS and GR. As shown in Fig. 2b, the accuracy of P_{theo} is evidenced by its consistency with the "true" values. Accordingly, we use P_{theo} below as a benchmark for the survival probability retrieved from every simulation result.

====================

Figure 2

====================

The measured survival probability of particles in a growing population can be estimated using $P_{n\log}$. Figure 2b shows that the decrease of $n_{\log}$ along the growth trajectory is consistent with the decreasing theoretical survival probability. This is because the width of the growing $n_{\log}$ peak maintains relatively constant in the logarithmic size scale (see Theory) and hence the decrease of the maximum $n_{\log}$ is mainly caused by the coagulation scavenging. In contrast, P_J and P_n underestimate the survival probability because they neglect the broadening of particle size distribution in the linear size scale. These underestimations can be estimated according to $n_{\log} = n \cdot \ln 10 \cdot d_{\text{p}}$. For instance, for a population of particles growing from 2 nm to 20 nm, P_J and P_n are expected to report survival probabilities that are approximately one order of magnitude (0.1 = 2 nm / 20 nm) lower than $P_{n\log}$.

The validity of $P_{n\log}$ for an ideal growing aerosol population can be generalized to the growth of atmospheric new particles, e.g., in a banana-type NPF event. Figure 2c shows a typical banana-type NPF event measured at Hyytiälä, with the formation of new particles around noon and a clean pattern of subsequent particle growth. The growth trajectory of new particles is indicated using the maximum concentration of particles measured in each size bin, with the maximum concentration mainly contributed by particles formed with the maximum formation rate (at noon) (Kulmala et al., 2012). For this NPF event, $P_{n\log}$ is consistent with the P_{theo} predicted using the measured CoagS and GR, whereas P_J and P_n substantially underestimate particle survival probability (Fig. 2d).

We then test the methods to retrieve the survival probability of particles from steady-state distributions. As shown in Fig. 3a, new particles in the simulated system are generated with a constant formation rate and they grow with a time-independent GR. The size-distribution of freshly nucleated particles reaches a steady state shortly after the initial state, though the whole system is at a pseudo-steady state with net production of large particles. Due to the continuous particle formation, it is difficult to apply the definition of survival probability in Eq. 1 to the simulated NPF. Misapplying Eq. 1 by taking all the measured particles as survived particles would result in a survival probability values larger than unity (Fig. 3b).

```
====================
```

Figure 3

```
250                 ====================
```

P_J and P_n are valid for particles with steady-state concentrations. For the simulated NPF in Fig. 3a, we compute P_J and P_n using the measured aerosol size distribution at the end of simulation ($t = 24$ h) instead of following a growth trajectory (see Eqs. 10 and 11). Consistent with the derivations in Theory, P_J can well reproduce P_{theo} with negligible uncertainties, and P_n is also a good estimate with minor uncertainties originated from the size-dependent GR. Accordingly, P_J and P_n in Eqs. 10-11

255   can be used for NPF with constant formation and growth rates, as well as freshly nucleated particles whose concentration is at a steady-state.

The validity of P_J and P_n for steady-state size distributions is verified using an NPF event measured in the CLOUD chamber. As shown in Fig. 3c, with a constant formation rate of freshly nucleated particles, the measured size distribution of sub-20 nm particles reached a steady state after an elapsed time of ~3 h. We took the size distribution measured at 3.5 h and computed P_J

260   and P_n using Eqs. 10-11. $P_{n\log}$ was also computed using the same size distribution. P_{theo} was computed using the measured GR and the total sink of particles. Instead of the CoagS, the sink of new particles in the CLOUD chamber was governed by dilution and size-dependent wall losses (Stolzenburg et al., 2020). For this NPF event, P_J and P_n is consistent with P_{theo} and $P_{n\log}$ overestimates the survival probability as it is expected (Fig. 3d).

Atmospheric NPF events are usually driven by precursors with varying concentrations. The growth of freshly nucleated

265   particles usually takes hours, whereas the particle formation rate usually varies significantly during such a long period, indicating that the steady-state assumption may not be valid for all particle sizes. As shown in Fig. 4a, freshly nucleated particles are formed between 0-5 h in a simulated system, and the nucleation rate as a function of time peaks at 2.5 h. These nucleated particles grow with a time-and-size independent GR. Fig. 4b shows the P_J in Eq. 10 with the steady-state assumption evaluated at $t = 2$, 3, and 4 h. Due to the varying GR, P_{theo} also varies with time. Comparing P_J and the corresponding P_{theo}

270   shows that the steady-state assumption is only valid for sub-5 nm particles in the simulated NPF, and the size range for this validity is even narrower at the beginning of NPF (e.g., $t = 2$ h).

```
====================
```

Figure 4

```
====================
```

275   We find that after considering the evolution of particle size distribution along the growth trajectory, P_J and P_n can provide good estimates of particle survival probability for the quasi-steady-state size distributions in Fig. 4a. Different from the results in Fig. 4b, we compute the P_J and P_n along the growth trajectory (using Eqs. 4 and 5, respectively) to account for the variation of J and n. As shown in Fig. 4c, the P_J and P_n along the growth trajectory are consistent with P_{theo} for sub-25 nm particles. When the quasi-steady-state is no long valid as particles on the trajectory grow above 25 nm, the growth of particle is similar

280   to the case in Fig. 2a and hence $P_{n\log}$ follows P_{theo} better than P_J and P_n in Fig. 4d.

The above analysis based on the simulated NPF is applicable to atmospheric NPF events measured in urban Beijing. As the example shown in Fig. 5a, intensive NPF were measured between 9:00 and 15:00 on an NPF day, forming a high concentration of new particles that grew subsequently to ~70 nm within the same day. A growth trajectory of new particles was obtained by tracking the fitted mode diameter of new particles. P_{theo} was predicted using the measured CoagS and GR, with the GR for

285   sub-5 nm particles corrected with the appearance time method (see Methods). With the high formation rate and high CoagS, it could be approximated that the size distribution of sub-10 nm particles was at a quasi-steady state. Accordingly, the P_J and P_n retrieved along the growth trajectory were consistent with P_{theo} in the sub-10 nm size range (Fig. 5d). For the growth of particles from 25 nm to larger sizes, P_{theo} was in better consistency with $P_{n\log}$ than P_n, since the measured growing size distribution was mainly contributed by the same population of new particles formed before 18:00.

290

=====================

Figure 5

=====================

To summarize, the survival probability of particles in a growing population can be retrieved using the measured $n_{\log}$ (Eq. 6), provided that the evolution of the size distribution is mainly caused by particle growth and scavenging losses. For quasi-steady-

295   state size distributions with continuous formation of new particles, the survival probability can be retrieved using J and n. Some atmospheric NPF events may be composed of quasi-steady-state size distributions with continuous particle formation and a subsequent growth of the new particle population, hence the survival probability can be estimated using a combination of P_n or P_J for small particles and $P_{n\log}$ for large particles.

4.2 Consistency between measured and theoretical survival probabilities based on long-term measurements in Beijing

300   With the formulae to retrieve particle survival probability as presented above, we investigate particle survival based on long-term measurements in urban Beijing. The measured survival probabilities of particles growing from 1.4 nm to 25 nm and from 25 nm to 100 nm were approximated by P_n and $P_{n\log}$, respectively. P_J of sub-10 nm particles was also computed. We combine different formulae because for most NPF events in urban Beijing, the size distribution of freshly nucleated particles is at a quasi-steady state whereas the formation rate of freshly nucleated particles is negligible when the growing particles are larger

305   than 25 nm.

With case-by-case and time- and size-resolved analysis, we find that the measured survival probability is on average consistent with the theoretical prediction. Fig. 6 shows the reconstructed median survival probabilities, for which the measured values characterized by P_n and $P_{n\log}$ are very consistent with P_{theo} for the whole size range from 1.4 nm to 100 nm. This consistency is also supported by the measured P_J of sub-10 nm particles, which is comparable to P_{theo}.

310

=====================

Figure 6

=====================

There has been a puzzle that how new particles could survive against the high CoagS in polluted megacities (e.g., Kulmala et al., 2017), as the CoagS therein was thought to be so high that it would scavenge nearly all the freshly nucleated particles. In

315 order to explain the observed frequent NPF events, the CoagS has been hypothesized to be ineffective such that the sticking probability between a new particle and a large particle (i.e., scavenger) would be significantly below unity (Kulmala et al., 2017). Alternatively, it has been hypothesized that the GR of freshly nucleated particles could be extremely high (> 100 nm h^{-1}) such that these particles could grow rapidly through the smallest sizes and become less vulnerable to coagulation scavenging (Wang et al., 2020). However, here we address this puzzle by showing the good consistency between the theoretical and

320 measured median survival probabilities of new particles from the cluster size (~1.4 nm) to the cloud condensation nucleus size (~100 nm). This closure evidences that assuming an effective CoagS, the survival of new particles in urban Beijing can on average be explained by theory with a GR similar to that in clean environments (< 10 nm h^{-1}). This consistency is also in accordance with our previous finding that NPF in urban Beijing tends to occur on days with low CoagS (Cai et al., 2017b), as particle survival probability on these days are expected to be orders of magnitude higher than the probability on haze days. For

325 instance, Kulmala et al. (2022) have shown that the survival probability decreases sharply as the CoagS increases above 0.01 s^{-1}.

4.3 Uncertainties in particle survival probabilities

Despite the consistency in terms of median values, large deviations are sometimes observed between the measured and theoretical survival probabilities (Fig. 6). These deviations are most significant for sub-5 nm particles. There might be other

330 causes for these deviations as have been discussed in literature (Kulmala et al., 2017; Wang et al., 2020), yet we herein report the reasons associated with the sensitivity of survival probability to uncertainties. Eq. 3 shows that the survival probability is a non-linear function of GR and CS, indicating that a small perturbation in GR or CS will propagate into a large variation of the survival probability. For example, the GR of sub-5 nm particles retrieved using the mode fitting method is systematically lower than the GR retrieved using the appearance time method with an average ratio of 1:3. This difference is most likely due

335 to the underestimation of the mode-fitting GR (see Methods) and hence we compute the P_{theo} of sub-5 nm particles using the appearance-time GR. As shown in Fig. 6, this systematic difference in GR with a factor of 3 corresponds to a >2 orders of magnitude difference in the median P_{theo}.

To further quantify the sensitivity of the survival probability to uncertainties, we plot the size-segregated survival probability as a function of CoagS and GR. The size-dependent CoagS is characterized by the condensation sink (CS) of sulfuric acid. As

340 shown in Fig. 7, the survival probability is most sensitive to uncertainties at small particles sizes and high CS/GR values, under which conditions particles are mostly vulnerable to coagulation scavenging. The sensitivity is herein defined as $dP_{theo}/d(CS/GR)$ and it can be readily computed using Eq. 3. For instance, for a 1 nm particle with CS/GR = 20 nm^{-1}, the sensitivity per nanometer growth is 10, indicating that a 1 % bias in CS/GR will lead to a 10 % bias in the P_{theo} for particle growth from 1 nm to 2 nm. Similarly, the same 1 % bias in CS/GR will lead to a 14 % bias in the overall P_{theo} for particle

345 growth until 100 nm, which also indicates that the P_{theo} of smallest particles are most sensitive to uncertainties. For urban

Beijing, NPF is usually observed with high CS/GR (Fig. 7a), hence the survival probability can be very sensitive to uncertainties, especially for freshly nucleated particles in the sub-5 nm size range under a high CS/GR value. Further discussions on the uncertainties in the CoagS and survival probability can be found in Tuovinen et al. (2020) and Tuovinen et al. (2022).

350

========================

Figure 7

========================

In addition to the uncertainties in P_{theo}, there may be variations in the measured survival probability due to the complex inhomogeneous atmosphere. The homogeneity approximation as required by Eqs. 4-6 (see methods) seems to be on average

355 valid for regional NPF events in urban Beijing, as indicated by the consistency of median measured and theoretical survival probabilities. However, the growth of atmospheric new particles from the cluster size to 100 nm takes hours (Fig. 6), during which period the measured aerosol size distribution may be significantly affected by transport. For some NPF events in urban Beijing, significant influences of transport on the measured survival probability are observed, which can be readily identified according to the abrupt changes in the measured aerosol size distributions. Besides atmospheric inhomogeneity, traffic

360 emissions and other sources may add to the uncertainties of the measured survival probabilities.

4.4 Implications on particle survival probability in measurements and models

The above analysis has shown that $P_{n\log}$ can be used to approximate the survival probability of particles in a growing population and that P_n and P_J can be used for quasi-steady-state size distributions. Compared to P_J which is retrieved from particle formation rates, $P_{n\log}$ and P_n can be readily obtained from the measured aerosol size distributions. Further, the validity of P_J in

365 atmospheric NPF is usually limited to sub-10 nm particles, as the population balance assumption for calculating the formation rate of large new particles (e.g., > 25 nm) is challenged by transport and emissions. In contrast, $P_{n\log}$ and P_n can provide the measured survival probabilities of large particles (e.g., up to 100 nm). However, for the sub-5 nm size range, P_J seems to be less sensitive to atmospheric variations than $P_{n\log}$ and P_n (see Fig. 6).

The validity of $P_{n\log}$, P_n, and P_J in different types of NPF events calls for an attention to retrieving the survival probability from

370 measurements and applying the survival probability in models. As we have shown in Fig. 2, applying P_n or P_J to a growing aerosol population would significantly underestimate the survival probability. Alternatively, improperly relating the formation rate and the survival probability might significantly underestimate the formation rate of large particles and could condensation nuclei. For example, Kerminen and Kulmala (2002) proposed that the formation rate of critical clusters (e.g., 1 nm) can be derived using the formation rate of the detected smallest particles (e.g., 3 nm) and the theoretical survival probability.

375 Assuming an accurateness of the CoagS and GR for P_{theo} evaluation, the derived formation rate of critical clusters is expected to be relatively accurate since the size distribution of freshly nucleated particles is usually at a quasi-steady state. The maximum systematic uncertainty in this derivation associated with the type of NPF events is no more than 3 nm / 1 nm = 3. However, if

one predicts the formation rate of cloud condensation nuclei using P_{theo} and the formation rate of critical clusters, the predicted formation rate may be underestimated by 1-2 orders of magnitude as the size distributions of large particles may not be at a steady-state.

The sensitivity of P_{theo} to measurement uncertainties also calls for accurate assessments of GR. We have shown that with carefully computed GR as well as CoagS, the P_{theo} in urban Beijing is, on average, consistent with the measured survival probability. However, if the GR was underestimated by a factor of three, the P_{theo} could be off by several orders of magnitude (e.g., in Fig. 6), largely affecting the estimated influences of NPF on the atmospheric environment. The consistency between the measured median theoretical and measured survival probability also provides a potential method to retrieve the median GR of new particles in different atmospheric environments. Practically, it may be challenging to accurately retrieve the GR from the measured aerosol size distributions or gaseous precursors, while the median GR retrieved from the measured survival probability may be used as a reference.

5 Summary and conclusions

We reported methods to retrieve the survival probability of atmospheric new particles from different types of new particle formation events and investigated the consistency between the measured survival probability and theoretical predictions. One new method based on the logarithmic size-scale distribution function $n_{\text{log}} = \text{d}N/\text{dlog}d_{\text{p}}$ and two conventional methods based on the new particle formation rate J and the linear size-scale distribution function $n = \text{d}N/\text{d}d_{\text{p}}$ were tested. A sectional aerosol kinetic model was used to generate simulated aerosol size distributions for testing these methods. The theoretical survival probability against coagulation scavenging predicted using the size-dependent coagulation sink and growth rate was first validated using the definition of the survival probability and it was then used as a benchmark.

Based on the simulation results and theoretical analysis, we found that n_{log} can be used to retrieve the measured survival probability from a growing aerosol population, whereas J or n can be used for quasi-steady-state size distributions that are significantly affected by the continuous formation of new particles. Misapplying J or n to a growing aerosol population will underestimate the survival probability. The above findings were supported by measured new particle formation events in urban Beijing, the Finnish boreal forest, and the CLOUD chamber. The size-distribution of sub-10 nm particles during NPF in urban Beijing were usually at a quasi-steady-state, hence the survival probability could be retrieved using n and J. The validity of n and J for survival probability computation was also found to be valid for the steady-state size distribution measured in a CLOUD chamber experiment. For NPF events in the Finnish boreal forest and the growth of particles larger than 25 nm in urban Beijing, the survival probability could be retrieved using n_{log}. Compared to the method based on J, the methods based on n and n_{log} have advantages in their convenience in terms of computation, less sensitivity to uncertainties, and the applicability to particles up to the cloud condensation nucleus size (e.g., 100 nm).

We finally compared the measured survival probability in urban Beijing retrieved properly using the above methods and the theoretical survival probability against coagulation scavenging. For 65 NPF events obtained from long-term measurements,

410 the measured and theoretical survival probabilities are on average consistent with each other in the 1.4-100 nm size range, though both are sensitive to measurement uncertainties and atmospheric variations.

Data and code availability

Data are available via the link https://doi.org/10.5281/zenodo.6704909. The code for simulating NPF is available in Li and Cai
415 (2020).

Author Contribution

R.C. designed the research; C.D. and J. Jiang collected the Beijing data; D.S., J. Kangasluoma, and M.K. collected the Hyytiälä data; D.S. collected the CLOUD data; R.C. and C.L. prepared the model and performed the simulations; R.C., J. Kangasluoma,
420 V.-M.K. and M.K. analyzed the data; R.C. wrote the paper with input from all co-authors.

Competing interests

The author declares no competing interests.

Acknowledgements

We acknowledge the following projects: ACCC Flagship funded by the Academy of Finland grant number 337549, Academy
425 professorship funded by the Academy of Finland (grant no. 302958), Academy of Finland projects no. 1325656, 311932, 316114, 332547, 325647, and 346370; "Quantifying carbon sink, CarbonSink+ and their interaction with air quality" INAR project funded by Jane and Aatos Erkko Foundation, the National Science Foundation of China (22188102 and 92044301), European Research Council (ERC) project ATM-GTP Contract No. 742206, Samsung PM2.5 SRP, the European Union's Horizon 2020 research and innovation programme Marie Sklodowska-Curie grant agreement no. 895875 ("NPF-PANDA")
430 and the Marie Skłodowska Curie ITN "CLOUD-MOTION" (764991), the Hungarian Research, Development and Innovation Office (K132254. Technical and scientific staff in BUCT/AHL are acknowledged.

References

Aalto, P., Hämeri, K., Becker, E., Weber, R., Salm, J., Mäkelä, J. M., Hoell, C., O'dowd, C. D., Hansson, H.-C., Väkevä, M., Koponen, I. K., Buzorius, G., and Kulmala, M.: Physical characterization of aerosol particles during nucleation events, Tellus B: Chemical and Physical
435 Meteorology, 53, 344-358, 10.3402/tellusb.v53i4.17127, 2001.
Cai, R., Chen, D.-R., Hao, J., and Jiang, J.: A miniature cylindrical differential mobility analyzer for sub-3 nm particle sizing, Journal of Aerosol Science, 106, 111-119, 10.1016/j.jaerosci.2017.01.004, 2017a.
Cai, R., Yang, D., Fu, Y., Wang, X., Li, X., Ma, Y., Hao, J., Zheng, J., and Jiang, J.: Aerosol surface area concentration: a governing factor in new particle formation in Beijing, Atmospheric Chemistry and Physics, 17, 12327-12340, 10.5194/acp-17-12327-2017, 2017b.

440   Cai, R., Li, C., He, X.-C., Deng, C., Lu, Y., Yin, R., Yan, C., Wang, L., Jiang, J., Kulmala, M., and Kangasluoma, J.: Impacts of coagulation on the appearance time method for new particle growth rate evaluation and their corrections, Atmospheric Chemistry and Physics, 21, 2287-2304, 10.5194/acp-21-2287-2021, 2021.

Cai, R., Häkkinen, E., Yan, C., Jiang, J., Kulmala, M., and Kangasluoma, J.: The effectiveness of coagulation sink of 3–10 nm atmospheric particles, Atmospheric Chemistry and Physics Discussions, in review, 10.5194/acp-2022-262, 2022.

445   Deng, C., Fu, Y., Dada, L., Yan, C., Cai, R., Yang, D., Zhou, Y., Yin, R., Lu, Y., Li, X., Qiao, X., Fan, X., Nie, W., Kontkanen, J., Kangasluoma, J., Chu, B., Ding, A., Kerminen, V., Paasonen, P., Worsnop, R. D., Bianchi, F., Liu, Y., Zheng, J., Wang, L., Kulmala, M., and Jiang, J.: Seasonal characteristics of new particle formation and growth in urban Beijing, Environmental Science and Technology, 54, 8547–8557, 10.1021/acs.est.0c00808, 2020.

Deng, C., Cai, R., Yan, C., Zheng, J., and Jiang, J.: Formation and growth of sub-3 nm particles in megacities: impacts of background 450   aerosols, Faraday Discussions, 226, 348-363, 10.1039/d0fd00083c, 2021.

Duplissy, J., Merikanto, J., Franchin, A., Tsagkogeorgas, G., Kangasluoma, J., Wimmer, D., Vuollekoski, H., Schobesberger, S., Lehtinen, K. E., Flagan, R. C., Brus, D., Donahue, N. M., Vehkamäki, H., Almeida, J., Amorim, A., Barmet, P., Bianchi, F., Breitenlechner, M., Dunne, E. M., Guida, R., Henschel, H., Junninen, H., Kirkby, J., Kürten, A., Kupc, A., Määttänen, A., Makhmutov, V., Mathot, S., Nieminen, T., Onnela, A., Praplan, A. P., Riccobono, F., Rondo, L., Steiner, G., Tome, A., Walther, H., Baltensperger, U., Carslaw, K. S., Dommen, 455   J., Hansel, A., Petäjä, T., Sipilä, M., Stratmann, F., Vrtala, A., Wagner, P. E., Worsnop, D. R., Curtius, J., and Kulmala, M.: Effect of ions on sulfuric acid-water binary particle formation: 2. Experimental data and comparison with QC-normalized classical nucleation theory, Journal of Geophysical Research: Atmospheres, 121, 1752– 1775, , 10.1002/2015JD023539, 2016.

Fu, Y., Xue, M., Cai, R., Kangasluoma, J., and Jiang, J.: Theoretical and experimental analysis of the core sampling method: Reducing diffusional losses in aerosol sampling line, Aerosol Science and Technology, 53, 793-801, 10.1080/02786826.2019.1608354, 2019.

460   Gordon, H., Kirkby, J., Baltensperger, U., Bianchi, F., Breitenlechner, M., Curtius, J., Dias, A., Dommen, J., Donahue, N. M., Dunne, E. M., Duplissy, J., Ehrhart, S., Flagan, R. C., Frege, C., Fuchs, C., Hansel, A., Hoyle, C. R., Kulmala, M., Kürten, A., Lehtipalo, K., Makhmutov, V., Molteni, U., Rissanen, M. P., Stozhkov, Y., Tröstl, J., Tsagkogeorgas, G., Wagner, R., Williamson, C., Wimmer, D., Winkler, P. M., Yan, C., and Carslaw, K. S.: Causes and importance of new particle formation in the present-day and preindustrial atmospheres, Journal of Geophysical Research: Atmospheres, 122, 8739-8760, 10.1002/2017jd026844, 2017.

465   Hari, P., and Kulmala, M.: Station for Measuring Ecosystem–Atmosphere Relations (SMEAR II), Boreal Environmental Research, 10, 315-322, 2005.

Heinritzi, M., Dada, L., Simon, M., Stolzenburg, D., Wagner, A. C., Fischer, L., Ahonen, L. R., Amanatidis, S., Baalbaki, R., Baccarini, A., Bauer, P. S., Baumgartner, B., Bianchi, F., Brilke, S., Chen, D., Chiu, R., Dias, A., Dommen, J., Duplissy, J., Finkenzeller, H., Frege, C., Fuchs, C., Garmash, O., Gordon, H., Granzin, M., El Haddad, I., He, X., Helm, J., Hofbauer, V., Hoyle, C. R., Kangasluoma, J., Keber, T., 470   Kim, C., Kürten, A., Lamkaddam, H., Laurila, T. M., Lampilahti, J., Lee, C. P., Lehtipalo, K., Leiminger, M., Mai, H., Makhmutov, V., Manninen, H. E., Marten, R., Mathot, S., Mauldin, R. L., Mentler, B., Molteni, U., Müller, T., Nie, W., Nieminen, T., Onnela, A., Partoll, E., Passananti, M., Petäjä, T., Pfeifer, J., Pospisilova, V., Quéléver, L. L. J., Rissanen, M. P., Rose, C., Schobesberger, S., Scholz, W., Scholze, K., Sipilä, M., Steiner, G., Stozhkov, Y., Tauber, C., Tham, Y. J., Vazquez-Pufleau, M., Virtanen, A., Vogel, A. L., Volkamer, R., Wagner, R., Wang, M., Weitz, L., Wimmer, D., Xiao, M., Yan, C., Ye, P., Zha, Q., Zhou, X., Amorim, A., Baltensperger, U., Hansel, A., 475   Kulmala, M., Tomé, A., Winkler, P. M., Worsnop, D. R., Donahue, N. M., Kirkby, J., and Curtius, J.: Molecular understanding of the suppression of new-particle formation by isoprene, Atmospheric Chemistry and Physics, 20, 11809-11821, 10.5194/acp-20-11809-2020, 2020.

Jiang, J., Chen, M., Kuang, C., Attoui, M., and McMurry, P. H.: Electrical Mobility Spectrometer Using a Diethylene Glycol Condensation Particle Counter for Measurement of Aerosol Size Distributions Down to 1 nm, Aerosol Science and Technology, 45, 510-521, 480   10.1080/02786826.2010.547538, 2011.

Kerminen, V.-M., Chen, X., Vakkari, V., Petäjä, T., Kulmala, M., and Bianchi, F.: Atmospheric new particle formation and growth: review of field observations, Environmental Research Letters, 13, 10.1088/1748-9326/aadf3c, 2018.

Kerminen, V. M., and Kulmala, M.: Analytical formulae connecting the "real" and the "apparent" nucleation rate and the nuclei number concentration for atmospheric nucleation events, Journal of Aerosol Science, 33, 609-622, 2002.

485   Kirkby, J., Curtius, J., Almeida, J., Dunne, E., Duplissy, J., Ehrhart, S., Franchin, A., Gagne, S., Ickes, L., Kurten, A., Kupc, A., Metzger, A., Riccobono, F., Rondo, L., Schobesberger, S., Tsagkogeorgas, G., Wimmer, D., Amorim, A., Bianchi, F., Breitenlechner, M., David, A., Dommen, J., Downard, A., Ehn, M., Flagan, R. C., Haider, S., Hansel, A., Hauser, D., Jud, W., Junninen, H., Kreissl, F., Kvashin, A., Laaksonen, A., Lehtipalo, K., Lima, J., Lovejoy, E. R., Makhmutov, V., Mathot, S., Mikkila, J., Minginette, P., Mogo, S., Nieminen, T., Onnela, A., Pereira, P., Petaja, T., Schnitzhofer, R., Seinfeld, J. H., Sipila, M., Stozhkov, Y., Stratmann, F., Tome, A., Vanhanen, J., Viisanen, 490   Y., Vrtala, A., Wagner, P. E., Walther, H., Weingartner, E., Wex, H., Winkler, P. M., Carslaw, K. S., Worsnop, D. R., Baltensperger, U., and Kulmala, M.: Role of sulphuric acid, ammonia and galactic cosmic rays in atmospheric aerosol nucleation, Nature, 476, 429-433, 10.1038/nature10343, 2011.

Korhonen, H., Kerminen, V.-M., Kokkola, H., and Lehtinen, K. E. J.: Estimating atmospheric nucleation rates from size distribution measurements: Analytical equations for the case of size dependent growth rates, Journal of Aerosol Science, 69, 13-20, 495   10.1016/j.jaerosci.2013.11.006, 2014.

Kuang, C., McMurry, P. H., and McCormick, A. V.: Determination of cloud condensation nuclei production from measured new particle formation events, Geophysical Research Letters, 36, L09822, 10.1029/2009gl037584, 2009.

Kuang, C., Riipinen, I., Sihto, S. L., Kulmala, M., McCormick, A. V., and McMurry, P. H.: An improved criterion for new particle formation in diverse atmospheric environments, Atmospheric Chemistry and Physics, 10, 8469-8480, 10.5194/acp-10-8469-2010, 2010.

500   Kulmala, M., Dal Maso, M., Mäkelä, J. M., Pirjola, L., Väkevä, M., Aalto, P., Miikkulainen, P., Hämeri, K., and O'dowd, C. D.: On the formation, growth and composition of nucleation mode particles, Tellus, 53, 479-490, 2001.

Kulmala, M., Vehkamäki, H., Petäjä, T., Dal Maso, M., Lauri, A., Kerminen, V.-M., Birmili, W., and McMurry, P. H.: Formation and growth rates of ultrafine atmospheric particles: a review of observations, Journal of Aerosol Science, 35, 143-176, 10.1016/j.jaerosci.2003.10.003, 2004.

505   Kulmala, M., Petäjä, T., Nieminen, T., Sipilä, M., Manninen, H. E., Lehtipalo, K., Dal Maso, M., Aalto, P. P., Junninen, H., Paasonen, P., Riipinen, I., Lehtinen, K. E., Laaksonen, A., and Kerminen, V. M.: Measurement of the nucleation of atmospheric aerosol particles, Nature protocols, 7, 1651-1667, 10.1038/nprot.2012.091, 2012.

Kulmala, M., Kontkanen, J., Junninen, H., Lehtipalo, K., Manninen, H. E., Nieminen, T., Petäjä, T., Sipilä, M., Schobesberger, S., Rantala, P., Franchin, A., Jokinen, T., Jarvinen, E., Äijälä, M., Kangasluoma, J., Hakala, J., Aalto, P. P., Paasonen, P., Mikkilä, J., Vanhanen, J.,
510   Aalto, J., Hakola, H., Makkonen, U., Ruuskanen, T., Mauldin, R. L., 3rd, Duplissy, J., Vehkamäki, H., Bäck, J., Kortelainen, A., Riipinen, I., Kurtén, T., Johnston, M. V., Smith, J. N., Ehn, M., Mentel, T. F., Lehtinen, K. E., Laaksonen, A., Kerminen, V.-M., and Worsnop, D. R.: Direct observations of atmospheric aerosol nucleation, Science, 339, 943-946, 10.1126/science.1227385, 2013.

Kulmala, M., Kerminen, V. M., Petaja, T., Ding, A. J., and Wang, L.: Atmospheric gas-to-particle conversion: why NPF events are observed in megacities?, Faraday Discuss, 200, 271-288, 10.1039/c6fd00257a, 2017.

515   Kulmala, M., Cai, R., Stolzenburg, D., Zhou, Y., Dada, L., Guo, Y., Yan, C., Petaja, T., Jiang, J., and Kerminen, V. M.: The contribution of new particle formation and subsequent growth to haze formation, Environ Sci Atmos, 2, 352-361, 10.1039/d1ea00096a, 2022.

Lehtinen, K. E. J., Dal Maso, M., Kulmala, M., and Kerminen, V.-M.: Estimating nucleation rates from apparent particle formation rates and vice versa: Revised formulation of the Kerminen–Kulmala equation, Journal of Aerosol Science, 38, 988-994, 10.1016/j.jaerosci.2007.06.009, 2007.

520   Lehtipalo, K., Leppä, J., Kontkanen, J., Kangasluoma, J., Franchin, A., Wimmer, D., Schobesberger, S., Junninen, H., Petäjä, T., Sipilä, M., Mikkilä, J., Vanhanen, J., Worsnop, D. R., and Kulmala, M.: Methods for determining particle size distribution and growth rates between 1 and 3 nm using the Particle Size Magnifier, Boreal Environment Research, 19, 215-236, 2014.

Li, C., and Cai, R.: Tutorial: The discrete-sectional method to simulate an evolving aerosol, Journal of Aerosol Science, 150, 105615, 10.1016/j.jaerosci.2020.105615, 2020.

525   Liu, J., Jiang, J., Zhang, Q., Deng, J., and Hao, J.: A spectrometer for measuring particle size distributions in the range of 3 nm to 10 μm, Frontiers of Environmental Science & Engineering, 10, 63-72, 10.1007/s11783-014-0754-x, 2016.

Liu, Y., Yan, C., Feng, Z., Zheng, F., Fan, X., Zhang, Y., Li, C., Zhou, Y., Lin, Z., Guo, Y., Zhang, Y., Ma, L., Zhou, W., Liu, Z., Dada, L., Dällenbach, K., Kontkanen, J., Cai, R., Chan, T., Chu, B., Du, W., Yao, L., Wang, Y., Cai, J., Kangasluoma, J., Kokkonen, T., Kujansuu, J., Rusanen, A., Deng, C., Fu, Y., Yin, R., Li, X., Lu, Y., Liu, Y., Lian, C., Yang, D., Wang, W., Ge, M., Wang, Y., Worsnop, D. R., Junninen,
530   H., He, H., Kerminen, V.-M., Zheng, J., Wang, L., Jiang, J., Petäjä, T., Bianchi, F., and Kulmala, M.: Continuous and comprehensive atmospheric observations in Beijing: a station to understand the complex urban atmospheric environment, Big Earth Data, 4, 295-321, 10.1080/20964471.2020.1798707, 2020.

McMurry, P. H.: New particle formation in the presence of an aerosol: rates, time scales, and sub-0.01 μm size distributions Journal of Colloid and Interface Science, 95, 72-80, 1983.

535   Pierce, J. R., and Adams, P. J.: Efficiency of cloud condensation nuclei formation from ultrafine particles, Atmospheric Chemistry and Physics, 7, 1367–1379, 10.5194/acp-7-1367-2007, 2007.

Qiao, X., Yan, C., Li, X., Guo, Y., Yin, R., Deng, C., Li, C., Nie, W., Wang, M., Cai, R., Huang, D., Wang, Z., Yao, L., Worsnop, D. R., Bianchi, F., Liu, Y., Donahue, N. M., Kulmala, M., and Jiang, J.: Contribution of Atmospheric Oxygenated Organic Compounds to Particle Growth in an Urban Environment, Environmental Science and Technology, 55, 13646-13656, 10.1021/acs.est.1c02095, 2021.

540   Stolzenburg, D., Steiner, G., and Winkler, P. M.: A DMA-train for precision measurement of sub-10 nm aerosol dynamics, Atmospheric Measurement Techniques, 10, 1639-1651, 10.5194/amt-10-1639-2017, 2017.

Stolzenburg, D., Simon, M., Ranjithkumar, A., Kürten, A., Lehtipalo, K., Gordon, H., Ehrhart, S., Finkenzeller, H., Pichelstorfer, L., Nieminen, T., He, X.-C., Brilke, S., Xiao, M., Amorim, A., Baalbaki, R., Baccarini, A., Beck, L., Bräkling, S., Caudillo Murillo, L., Chen, D., Chu, B., Dada, L., Dias, A., Dommen, J., Duplissy, J., El Haddad, I., Fischer, L., Gonzalez Carracedo, L., Heinritzi, M., Kim, C., Koenig,
545   T. K., Kong, W., Lamkaddam, H., Lee, C. P., Leiminger, M., Li, Z., Makhmutov, V., Manninen, H. E., Marie, G., Marten, R., Müller, T., Nie, W., Partoll, E., Petäjä, T., Pfeifer, J., Philippov, M., Rissanen, M. P., Rörup, B., Schobesberger, S., Schuchmann, S., Shen, J., Sipilä, M., Steiner, G., Stozhkov, Y., Tauber, C., Tham, Y. J., Tomé, A., Vazquez-Pufleau, M., Wagner, A. C., Wang, M., Wang, Y., Weber, S. K., Wimmer, D., Wlasits, P. J., Wu, Y., Ye, Q., Zauner-Wieczorek, M., Baltensperger, U., Carslaw, K. S., Curtius, J., Donahue, N. M., Flagan, R. C., Hansel, A., Kulmala, M., Lelieveld, J., Volkamer, R., Kirkby, J., and Winkler, P. M.: Enhanced growth rate of atmospheric particles
550   from sulfuric acid, Atmospheric Chemistry and Physics, 20, 7359-7372, 10.5194/acp-20-7359-2020, 2020.

Tuovinen, S., Kontkanen, J., Jiang, J., and Kulmala, M.: Investigating the effectiveness of condensation sink based on heterogeneous nucleation theory, Journal of Aerosol Science, 149, 105613, 10.1016/j.jaerosci.2020.105613, 2020.

Tuovinen, S., Cai, R., Kerminen, V.-M., Kulmala, M., and Kontkanen, J.: Survival probabilities of atmospheric particles: comparison based on theory, cluster population simulations, and observations from Beijing, in preparation, 2022.

555 Wang, M., Kong, W., Marten, R., He, X. C., Chen, D., Pfeifer, J., Heitto, A., Kontkanen, J., Dada, L., Kurten, A., Yli-Juuti, T., Manninen, H. E., Amanatidis, S., Amorim, A., Baalbaki, R., Baccarini, A., Bell, D. M., Bertozzi, B., Brakling, S., Brilke, S., Murillo, L. C., Chiu, R., Chu, B., De Menezes, L. P., Duplissy, J., Finkenzeller, H., Carracedo, L. G., Granzin, M., Guida, R., Hansel, A., Hofbauer, V., Krechmer, J., Lehtipalo, K., Lamkaddam, H., Lampimaki, M., Lee, C. P., Makhmutov, V., Marie, G., Mathot, S., Mauldin, R. L., Mentler, B., Muller, T., Onnela, A., Partoll, E., Petaja, T., Philippov, M., Pospisilova, V., Ranjithkumar, A., Rissanen, M., Rorup, B., Scholz, W., Shen, J., Simon,
560 M., Sipila, M., Steiner, G., Stolzenburg, D., Tham, Y. J., Tome, A., Wagner, A. C., Wang, D. S., Wang, Y., Weber, S. K., Winkler, P. M., Wlasits, P. J., Wu, Y., Xiao, M., Ye, Q., Zauner-Wieczorek, M., Zhou, X., Volkamer, R., Riipinen, I., Dommen, J., Curtius, J., Baltensperger, U., Kulmala, M., Worsnop, D. R., Kirkby, J., Seinfeld, J. H., El-Haddad, I., Flagan, R. C., and Donahue, N. M.: Rapid growth of new atmospheric particles by nitric acid and ammonia condensation, Nature, 581, 184-189, 10.1038/s41586-020-2270-4, 2020.

Weber, R. J., Marti, J. J., McMurry, P. H., Eisele, F. L., Tanner, D. J., and Jefferson, A.: Measurements of new particle formation and
565 ultrafine particle growth rates at a clean continental site, Journal of Geophysical Research: Atmospheres, 102, 4375-4385, 10.1029/96jd03656, 1997.

Zhang, R., Khalizov, A., Wang, L., Hu, M., and Xu, W.: Nucleation and growth of nanoparticles in the atmosphere, Chemical Reviews, 112, 1957-2011, 10.1021/cr2001756, 2012.

570

Table 1: Simulation conditions for Figs. 2-4.

Figure No.	Formation rate	Steady state?	Self-coagulation?
2	0	No	No
3	Constant	Yes	No
4	Varying	Quasi-steady-state for freshly nucleated particles	Yes
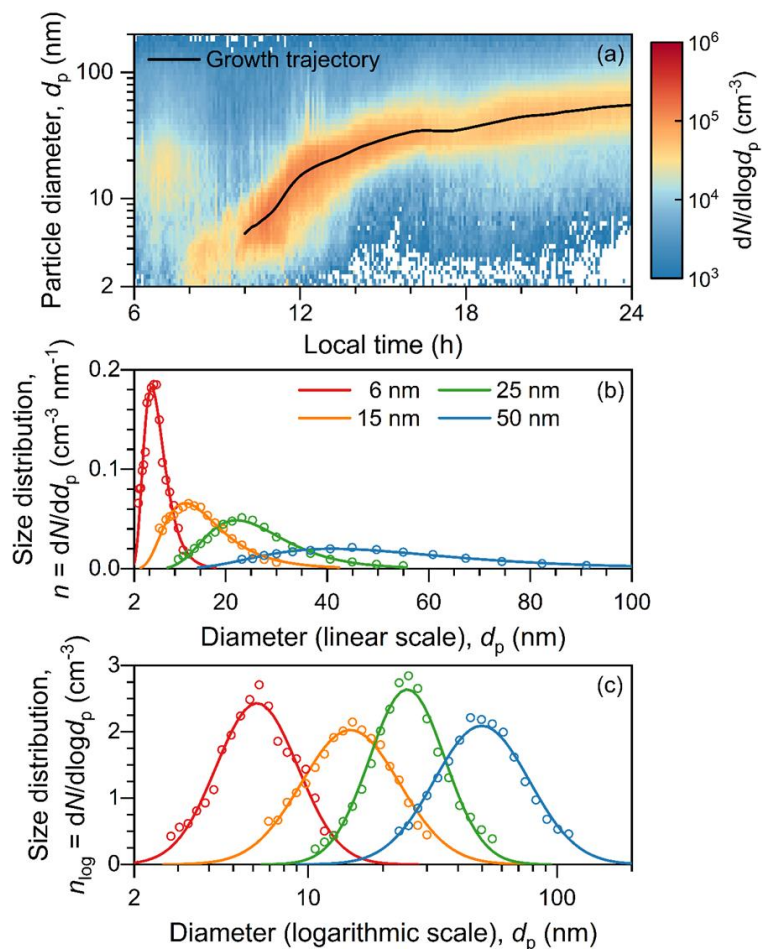
575 **Figure 1: Evolution of aerosol size distribution in urban Beijing during an NPF event.** Panel (a) shows the whole growth pattern and panels (b) and (c) shows the dN/dd_p and $dN/d\log d_p$, respectively, when growing new particles reached certain sizes. In panels (b) and (c), the size distribution has been normalized by dividing it by the fitted number concentration so that the area of every peak is equal to unity. The markers and lines are the measured and fitted distributions, respectively. The size distributions in panels (b) and (c) are identical to each other, though they are shown in different vertical axes and horizontal scales.
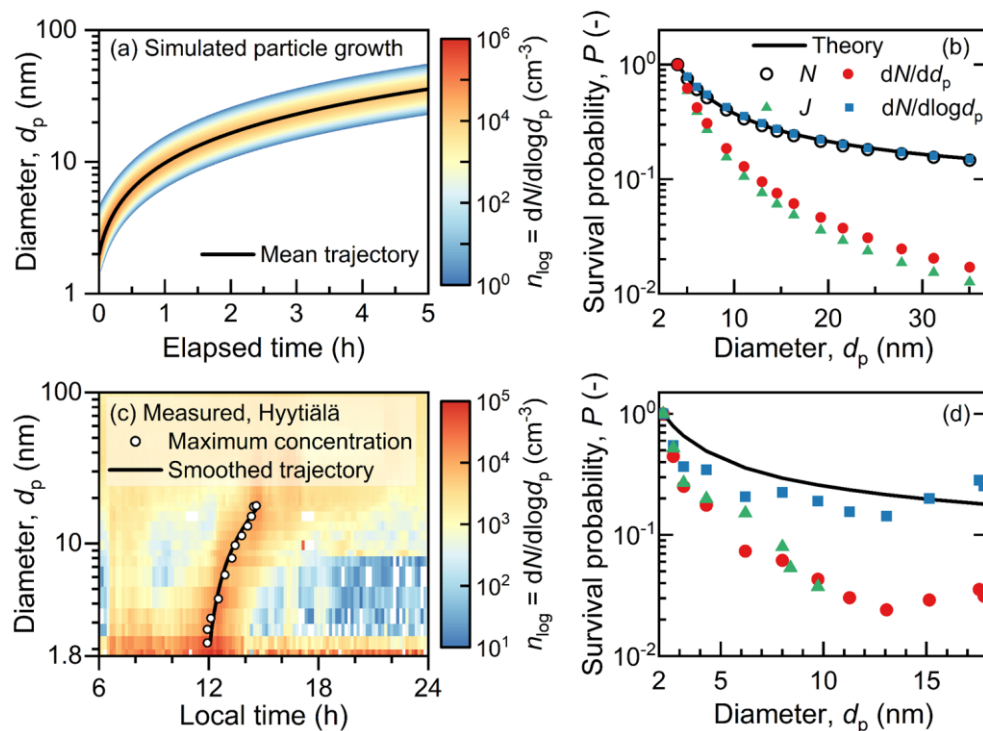
Figure 2: Survival probabilities of new particles in simulated and measured growing aerosol populations. (a) A growing size distribution of an aerosol population. There is no formation of new particles after the initial state. (b) The survival probability of new particles in the simulated aerosol population retrieved using different methods. (c) A banana-type NPF event measured from the boreal environment at Hyytiälä. A growth trajectory is retrieved using the maximum concentration method (Kulmala et al., 2012). (d) The survival probability of new particles in the measured NPF event. The theoretical lines in panels (b) and (d) are retrieved from the growth rate and the coagulation sink using Eqs. 2-3. The markers show the survival probabilities retrieved from the size distribution using Eqs. 1 and 4-6. Briefly, the retrieved survival probability is equal to $X(d_{p2})/X(d_{p1})$, where X is N, dN/dd_p, J, or $dN/dlogd_p$.
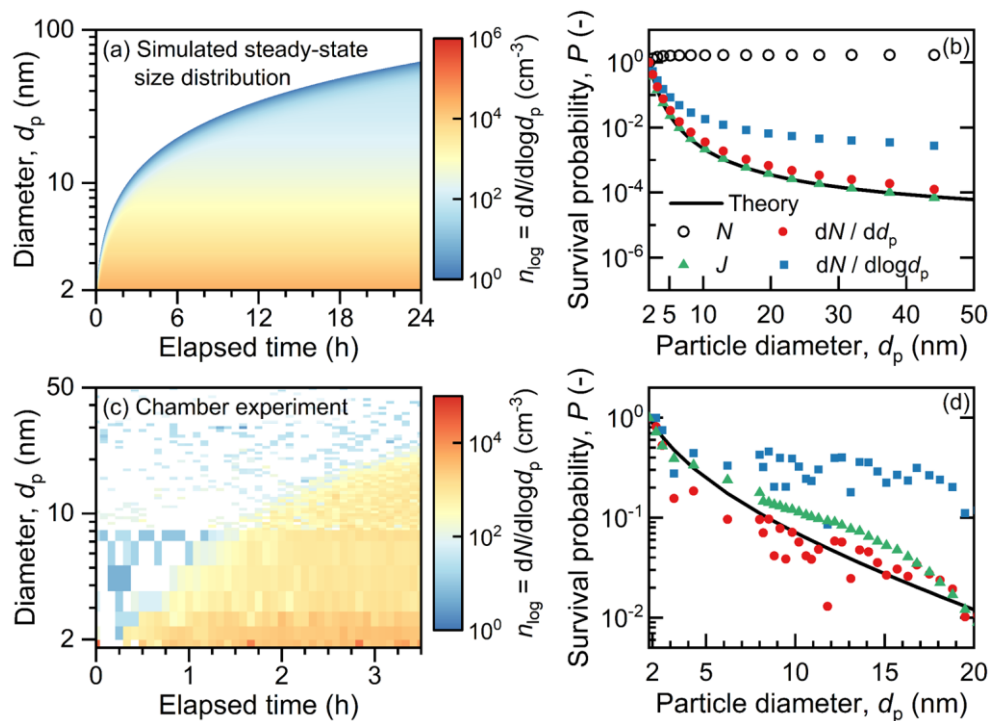
590 **Figure 3: Survival probabilities of new particles with steady-state size distributions.** (a) Simulated size distribution of new particles. The formation and size-dependent growth rates of particles are maintained constant during the simulation. (b) The survival probability of new particles in the simulated new particle formation event retrieved using different methods. N is herein the total number concentration of particles. (c) An NPF event measured in the CLOUD chamber. (d) The survival probability of new particles in the measured NPF event evaluated at 3.5 h elapsed time.

595
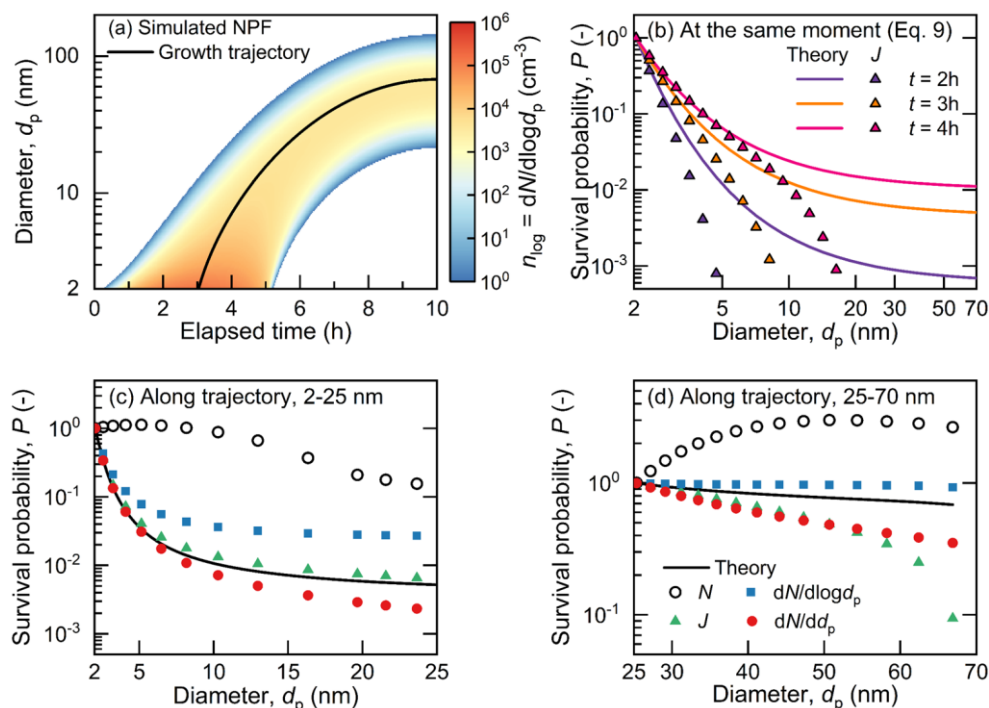
Figure 4: Survival probabilities of new particles in an NPF event with varying formation and growth rates. (a) Simulated size distribution of new particles. (b) The survival probabilities of new particles retrieved using Eq. 10 for steady-state size distributions at 2 h, 3 h and 4 h elapsed time (t). Theoretical survival probabilities evaluated the corresponding time are also shown. (c) The survival probability of 2-25 nm particles following the growth trajectory. N is the total number of particles. (d) The survival probability of 25-70 nm particles following the growth trajectory.
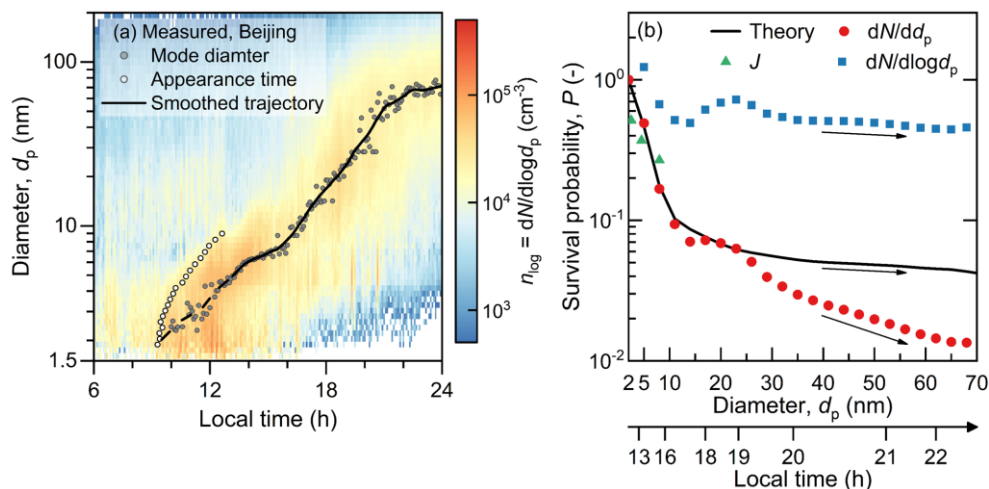
Figure 5: Survival probabilities of new particles in a measured new particle formation event in urban Beijing. (a) Measured size distribution of new particles. The growth trajectory is determined using the mode-fitting method (Kulmala et al., 2012). For sub-5 nm particles, the mode-fitting method is likely to underestimate the grow rate (see Methods), as indicated by its different slope from the trajectory retrieved using the appearance time method (Lehtipalo et al., 2014). (b) The measured and theoretical survival probabilities of new particles along the trajectory. The theoretical survival probability of sub-5 nm particles has been corrected using the growth rate reported by the appearance time method. The arrows indicate the trend of the survival probability of 25-70 nm particles. A non-linear axis shows the local time corresponding to the growing particle size, indicating potential atmospheric variations during the growth of new particles.

610
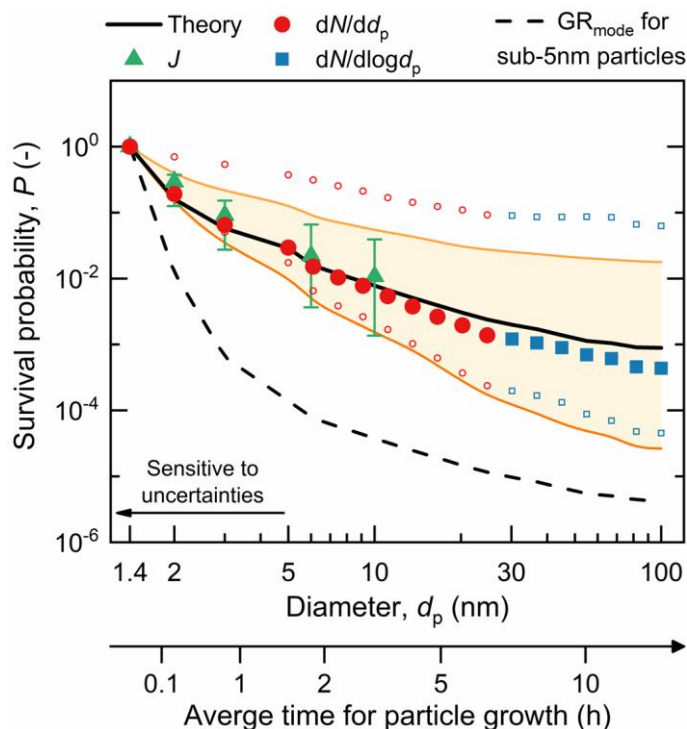
Figure 6: Measured and theoretical survival probabilities of new particles in urban Beijing. The markers and lines shows the median survival probability obtained from 65 NPF events. The variation bars, open markers, and the shaded area indicates the 25 % - 75 % variation range of the survival probabilities computed using J, dN/dd_p or $dN/dlogd_p$, and theory, respectively. The difference between the solid and dashed lines for theoretical survival probabilities is caused by the difference between the sub-5 nm particle growth rate retrieved using the appearance time method and the mode fitting method. A non-linear horizontal axis shows the local time corresponding to the growing particle size, indicating atmospheric variations during the measured new particle formation and growth.
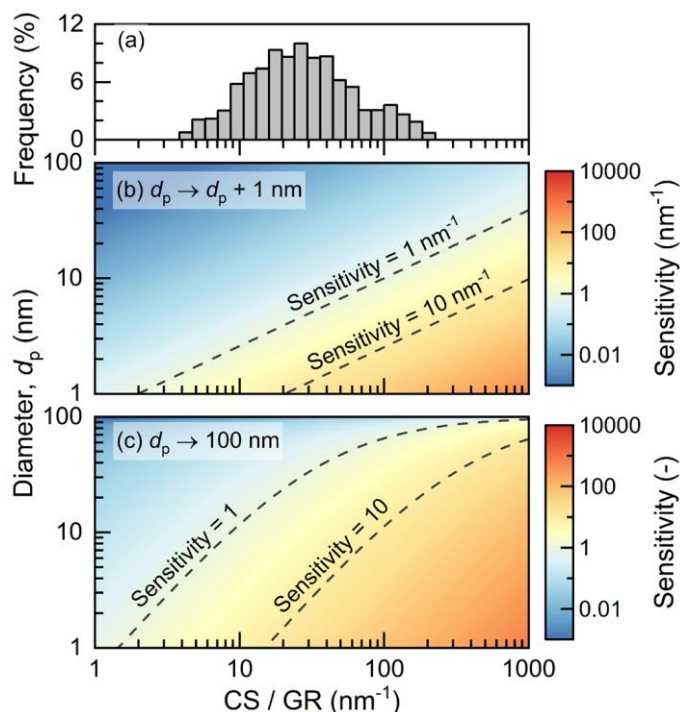
Figure 7: Sensitivity of the survival probability to particle growth rate (GR) and the coagulation sink. The size-dependent coagulation sink is characterized using the condensation sink (CS) the sulfuric acid. The sensitivity is defined as the relative change of survival probability per relative change of CS/GR. For instance, sensitive = 1 indicates that a 1 % relative change in CS/GR will result in the same relative change in the survival probability. (a) The frequency distribution of CS/GR in the measured NPF events in urban Beijing, with the frequency indicated by the height of each bar. (b) The sensitivity of the survival probability of particles growing by 1 nm. (c) The sensitivity of the survival probability of particles growing to 100 nm.